Effect of Fluorination and Size of the Alkyl Side-Chain on the Solubility of Carbon Dioxide in 1-Alkyl-3-methylimidazolium Bis(trifluoromethylsulfonyl)amide Ionic Liquids

D. Almantariotis,[†] T. Gefflaut,[†,‡] A. A. H. Pádua,[†] J.-Y. Coxam,[†] and M. F. Costa Gomes*,[†]

Laboratoire de Thermodynamique et Interactions Moléculaires, CNRS UMR 6272, Synthèse et Etudes de Systèmes à Intérêt Biologique, CNRS UMR 6504 and Clermont Université, Université Blaise Pascal, Clermont-Ferrand, 24, avenue des Landais, 63177 Aubière Cedex, France

It is proven in this work that it is possible to significantly increase the carbon dioxide uptake by an ionic liquid relying on physical interactions only. The solubility and thermodynamics of solvation of carbon dioxide in the ionic liquids 1-octyl-3-methylimidazolium bis[trifluoromethylsulfonyl]amide [C_8mim][Ntf_2], 1-decyl-3-methylimidazolium bis[trifluoromethylsulfonyl]amide [C_{10}mim][Ntf_2], and 1-(3,3,4,4,5,5,6,6,7,7,8,8,8-tridecafluorooctyl)-3-methylimidazolium bis[trifluoromethylsulfonyl]amide [$C_8H_4F_{13}$mim][Ntf_2] were determined experimentally between 298 and 343 K at pressures close to atmospheric. The solubility of carbon dioxide is significantly higher in the fluorine-substituted ionic liquid with Henry's law constants at 303 K of 33.3 and 30.7 bar for [C_8mim][Ntf_2] and [C_{10}mim][Ntf_2], respectively, and of 28.0 bar for [$C_8H_4F_{13}$mim][Ntf_2]. Molecular simulation was used for interpreting the molecular mechanisms of solvation of carbon dioxide in the studied ionic liquids and coherent molecular mechanisms of solvation are proposed in light of the solute−solvent radial distribution functions. It is shown that the increase of the size of the hydrogenated or fluorinated alkyl chain in the imidazolium cation does not lead to a steady augmentation of the gaseous uptake by the liquid probably due to an increase of the nonpolar domains of the ionic liquid, carbon dioxide being solvated preferentially in the charged regions of the solvent.

Introduction

Conventional processes for carbon dioxide removal from flue-gas streams include a chemical and/or physical process.[1] The chemical absorption-based processes that involve the use of aqueous solutions of amines with high absorption capacity, require intensive energy use for solvent regeneration and present serious corrosion issues.[2,3] Furthermore, the amine solutions are not thermally stable and show a non-negligible volatility leading to important absorbent losses during regeneration. The research of promising physical absorbents, implies the investigation of stable compounds as solvents for selective CO_2 capture at extended ranges of pressures and temperatures, representative of gasification conditions. The regeneration of the solvent is an important issue and can be addressed both by using pressure swing or thermal swing processes, the first being interesting in the cases where the absorption is made at high temperatures, eliminating the necessity of cooling down the gas-stream prior to the absorption operation.

Among the most studied alternative physical absorbents for carbon dioxide are perfluorinated organic liquids,[1,4] which are chemically very stable, have high-boiling points, high densities, and elevated molecular weights. Their molecular structures are dominated by the very strong C−F bonds, causing an increase in rigidity and a decrease in polarity.[4] These unique properties lead to high gas solubility,[5−7] medium vapor losses,[8] and low forces required for expelling the gas molecules and regenerating the solvent either upon decreasing pressure or increasing temperature.

Ionic liquids are considered as promising alternatives as media for the capture of carbon dioxide.[1,3] They address most of the inconvenients of using aqueous solutions of amines and, compared with other possible physical absorbents, do not evaporate, are often thermally and chemically stable and seem to have a very low environmental impact. The physicochemical properties of ionic liquids (including their carbon dioxide absorption capacity) can be tuned by appropriately combining different cations and anions or by choosing appropriate cation/anion pairs and modify them, introducing chemical features that will render the ionic liquid specific for a given task.[9] This is not always a straightforward assignment as, although we are generally able to obtain a new ionic liquid, the properties of these complex fluids can vary dramatically, sometimes in unexpected directions, even when small modifications are included on their molecular structure.

In this work, we have decided to combine the interesting properties of two classes of chemicals, ionic liquids and fluorous phases, and create new ionic liquids that hopefully will exhibit a larger capacity to absorb carbon dioxide.[4] This approach has been tried before by Baltus et al.[10] and Muldoon et al.[11] who have published values of the low pressure solubility of carbon dioxide in 1-methyl-3−3,3,4,4,5,5,6,6,7,7,8,8,8-tridecafluoro-octyl)imidazolium bis[(trifluoromethyl)sulfonyl]amide ([C_8H_4-F_{13}mim][NTf_2]). Their results on the solubility of carbon dioxide differ by more than 80% in Henry's law constant and no solvation mechanism is proposed to explain the dissolution of the gas in the ionic liquid. Muldoon et al.[11] addressed the differences encountered by measuring the carbon dioxide solubility using different experimental techniques. The carbon dioxide solubility in [$C_8H_4F_{13}$mim][NTf_2] is consistent with the one measured in a similar ionic liquid synthesized by the authors, the 1-methyl-3−3,3,4,4,5,5,6,6,6-nonafluorohexyl)imidazolium

* To whom correspondence should be addressed. E-mail: Margarida.c. gomes@univ-bpclermont.fr.
† Laboratoire de Thermodynamique et Interactions Moléculaires.
‡ Synthèse et Etudes de Systèmes à Intérêt Biologique.

Fluorination and Solubility of CO₂ in Ionic Liquids

J. Phys. Chem. B, Vol. 114, No. 10, 2010 **3609**
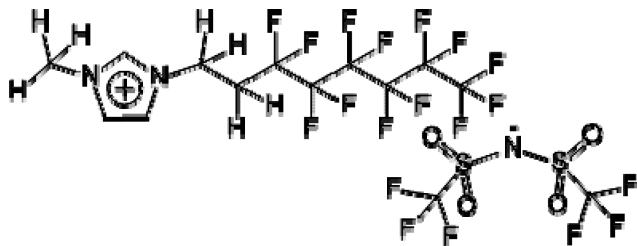
Figure 1. Chemical structure of the ionic liquid 1-(3,3,4,4,5,5,6,6,7,7,8,8,8-tridecafluorooctyl)-3-methylimidazolium bis[trifluoromethylsulfonyl]amide [C₈H₄F₁₃mim][NTf₂].

bis[(trifluoromethyl)sulfonyl]amide ([C₆H₄F₉mim][NTf₂]). Muldoon et al.[11] have concluded that the published values by Baltus et al.,[10] measured using a quartz crystal microbalance, substantially overestimate the carbon dioxide solubility in this ionic liquid. We report herein new data for the low-pressure solubility of carbon dioxide in the partially fluorinated ionic liquid as a function of temperature, and we use molecular simulation to assess the molecular mechanisms of solvation in the partially fluorinated ionic liquid and how it differs from the solvation in the equivalent 1-alkyl-3-methylimidazolium based ionic liquid, namely in 1-octyl-3-methylimidazolium bis[trifluoromethylsulfonyl]amide and in 1-decyl-3-methylimidazolium bis[trifluoromethylsulfonyl]amide.

Experimental Section

Materials. The gas used for the solubility measurements was carbon dioxide from AGA/Linde Gaz, with mole fraction purity of 0.99995. The gas was used as received from the manufacturer.

The samples of 1-octyl-3-methylimidazolium bis[trifluoromethylsulfonyl]amide ([C₈mim][NTf₂]) and 1-decyl-3-methylimidazolium bis[trifluoromethylsulfonyl]amide ([C₁₀mim][NTf₂]) were supplied by the laboratories at the Queens University of Belfast. The minimum stated mole fraction purity is 0.99. A volumetric Karl Fischer titration using a Mettler Toledo DL31 titrator was used for determining the water content of an ionic liquid sample kept under a primary vacuum during at least 24 h. The value found was of 110 and 115 ppm for [C₈mim][NTf₂] and [C₁₀mim][NTf₂], respectively. The halide content of the ionic liquid was determined using suppressed ion chromatography (IC) and it was found to be less than 5 ppm of chloride in both samples.

Room-temperature ionic liquid 1-(3,3,4,4,5,5,6,6,7,7,8,8,8-tridecafluorooctyl)-3-methylimidazolium bis[trifluoromethylsulfonyl]amide ([C₈H₄F₁₃mim][NTf₂]) is represented in Figure 1 and was synthesized using the procedure described in literature.[12,13] The precursors used for this synthesis were 1-methylimidazole, purchased from Fluorochem with a mole fraction purity of 0.99; 1,1,1,2,2,3,3,4,4,5,5,6,6-tridecafluoro-8-iodooctane, purchased from Fluorochem with a mole fraction purity 0.97; and lithium bis[trifluoromethanesulfonyl]amide salt, purchased from Fluka, puriss. >99%. All solvents used are of analytical grade.

In a 250 mL round-bottomed flask under argon, toluene (approximately 60 mL) and freshly distilled 1-methyl-imidazole (6.52 g or 79.41 mmol) were introduced with the mixture being heated up to 60 °C under agitation. 1,1,1,2,2,3,3,4,4,5,5,6,6-Tridecafluoro-8-iodooctane (41.44 g or 87.42 mmol) in 10 mol % excess was then slowly added while stirring over 30 min with the reaction mixture being kept under reflux at 60 °C for 5 days. After cooling with an ice bath, the product was filtered and washed with toluene and diethyl ether, before being kept under vacuum (0.1 mmHg) at 40 °C for 48 h. A yellow solid

product was obtained and was identified as being 1-(3,3,4,4,5,5,6,6,7,7,8,8,8-tridecafluorooctyl)-3-methyl-imidazolium iodide ([C₈H₄F₁₃mim][I]) (23.86 g or 42.90 mmol, 54% global yield).

This solid (23.86 g or 42.90 mmol) was then dissolved in approximately 400 mL of water, and the solution was heated to 60 °C before the dropwise addition of lithium bis(trifluoromethanesulfonyl)amide (12.95 g or 45.13 mmol) in 5 mol % excess. After 10 min at 60 °C, the mixture was cooled to room temperature and the product was extracted with dichloromethane. The water was decanted and the organic phase was then washed with water until no iodide was detected using a silver nitrate test. The product obtained in dichloromethane solution was further purified using an (activated charcoal + neutral alumina) column. After drying under a vacuum of 0.1 mmHg at 40 °C for 48 h, a slight-yellow product was obtained and was identified as being the 1-(3,3,4,4,5,5,6,6,7,7,8,8,8-tridecafluorooctyl)-3-methylimidazolium bis[trifluoromethylsulfonyl]amide ([C₈H₄F₁₃mim][NTf₂]) (37.41 mmol, global yield of 87%).

The minimum mole fraction purity is 0.99, as found by ¹H and ¹⁹F NMR spectrometry (the NMR data are reported in the Supporting Information). A coulometric Karl Fisher titration (model Mettler Toledo DL32, standard method KF) was used to determine the water content of the sample, which is less than 90 ppm. The iodide ion content was found to be less than 400 ppm as determined by ionic chromatography.

The study of the phase transition and decomposition temperatures for [C₈H₄F₁₃mim][NTf₂] shows a melting point temperature bellow −50 °C (or 223.15 K). Additionally, it possesses extremely high thermal stability, its thermal decomposition being detected in this work, using differential scanning calorimetry (DSC, Modulated 2920, TA Instruments), at 368 °C (or 638.15 K). As a comparison, [C₈mim][NTf₂] also presents a low melting point temperature, −84 °C (or 189.15 K), but a slightly lower temperature of decomposition, 345 °C (or 618.15 K)[37] than the [C₈H₄F₁₃mim][NTf₂].

The samples of the ionic liquids were kept under primary vacuum for at least 24 h at 303 K before each measurement.

Density Measurements. Densities were measured using a U-shaped vibrating-tube densimeter (Anton Paar, model DMA 512) operating in a static mode, following the procedure described in previous publications.[14,15] Measurements for [C₈H₄F₁₃mim][NTf₂] were performed for pressures up to 25 MPa and temperatures from 293 to 343 K and for [C₈mim][NTf₂] and [C₁₀mim][NTf₂] only at atmospheric pressure and temperatures from 308 to 333 K.

The temperature was maintained constant to within ±0.01K by means of a recirculating bath equipped with a PID temperature controller (Julabo FP40-HP). For measuring the temperature, a 100 Ohm platinum resistance thermometer (precision of ±0.02 K and accuracy of ±0.04 K) was used. Its calibration was performed by verifying a water triple point (triple point cell by Hart Scientific) and by comparison against a 100 Ohm platinum resistance Hart Scientific model 1502A. The pressure was measured using a precision pressure transmitter Druck, model PTX 610, working in a range from 0 to 70 MPa with an uncertainty 0.08% full scale.

The measured period of vibration (τ) of a U tube is related to the density (ρ) according to $\rho = A\tau^2 + B$ where A and B are parameters that are function of temperature and pressure determined by calibration between temperatures of 293 and 343 K and pressures of 0.1 and 25 MPa, using as calibration fluids *n*-heptane, bromobenzene, and 2,4-dichlorotoluene following the recommendations by Schilling et al.[16] Density measurements
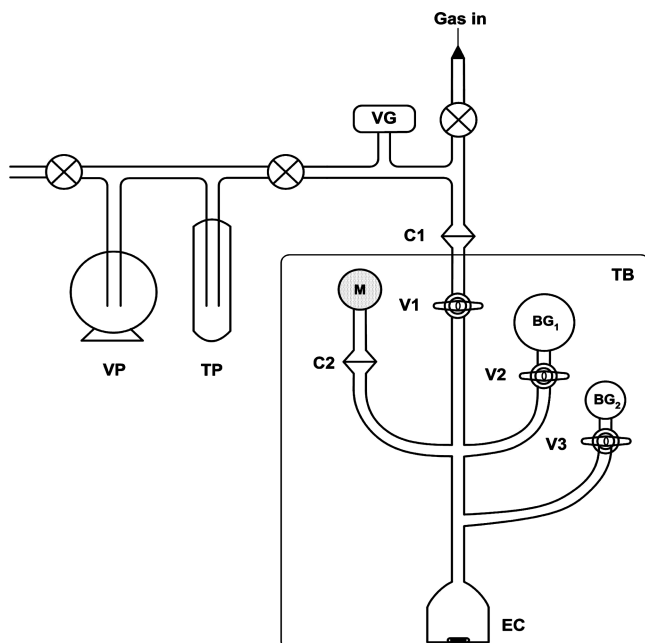
Figure 2. Solubility apparatus used in this work. VP, vacuum pump; TP, cold trap; VG, vacuum gauge; M, precision manometer; BG$_1$, BG$_2$, glass bulbs; TB, thermostatted liquid bath; EC, equilibrium cell; V1, V2, V3, constant volume glass valves; C1, C2, vacuum O-ring connections.

were performed in steps of 10 K and at 10 different pressures from 0.1 to 25 MPa. The uncertainty of the density measurement is estimated as 10^{-4} g cm^{-3}.[15]

Because of the high viscosity of both ionic liquids used during this work (at ambient conditions $\eta > 100$ mPa·s), there are systematic deviations on the density measurements depending on the fluid viscosity. Using the available correlations from Anton Paar,[17] corrections have been made considering the viscosity of the ionic liquid samples.

Viscosity Measurements. The dynamic viscosities of [C$_8$H$_4$F$_{13}$mim][NTf$_2$] and [C$_8$mim][NTf$_2$] previously dried under vacuum were measured using an Anton Paar AMVn rolling ball viscosimeter, as a function of the temperature from 293.15 to 363.15 K (controlled to within 0.01 K and measured with an accuracy better than 0.05 K) and at atmospheric pressure. Before starting the measurements, the 3 mm diameter capillary tube was calibrated as a function of temperature and angle of measurement using a standard viscosity oil from Cannon (N35). The overall uncertainty on the viscosity is estimated as ±1.5%.

Gas-Solubility Measurements. The experimental apparatus used for the present gas solubility measurements was based on an isochoric saturation technique and has been described in previous publications.[18−20] In this technique, a known quantity of gaseous solute is put in contact with a precisely determined quantity of degassed solvent at a constant temperature inside an accurately known volume. When thermodynamic equilibrium is attained, the pressure above the liquid solution is constant and is directly related to the solubility of the gas in the liquid.

The experimental apparatus used is schematically represented in Figure 2. The equilibrium cell EC, together with the precision pressure transducer M and the glass bulbs limited by valves V2 and V3, are the equilibrium section of the apparatus. The design of the equilibrium cell is very appropriate for the study of viscous liquid solvents like the ionic liquids measured in this work. The equilibrium cell permits the handling of volumes of liquid solvent varying from 3 to 6 mL and an appropriate gas/

liquid contact is guaranteed by means of good agitation using a glass-coated magnetic stirrer. The whole equilibrium section is maintained inside a approximately 500 L double water bath at constant temperature to within ±0.01 K using two PID temperature controllers and accurately measured with a calibrated 100 Ω platinum resistance thermometer from Hart Scientific (Hart Scientific model 1502A, accuracy of ±0.018 at 0 °C).

The solubility measurement starts with the introduction of a known quantity of gas solute in one or both of the calibrated glass bulbs limited by valves V2 and V3. The exact amount of gas is determined by measuring its pressure in the pressure transducer M (Druck RPT 350, 35−3500 mbar, precision of 0.01% full scale) at constant temperature, correcting for gas imperfections. The exact volume of both bulbs, which is significantly different (BG$_1$ = (55.14 ± 0.001) cm^3 at 303.38 K and BG$_2$ = (27.31 ± 0.002) cm^3 at 304.71 K), was previously calibrated with a precision better than ±0.1% at two different temperatures in order to appropriately take into account for the corrections due to thermal expansion (the value for the gas bulbs thermal expansion coefficient determined experimentally equals those of Pyrex glass found in the literature, $\alpha = 2.76 \times 10^{-5}$). The gas is isolated from the rest of the installation by closing the glass valves V2 and V3.

The ionic liquid is then introduced in the equilibrium cell through connection C2 by means of a syringe. The mass of ionic liquid introduced, which varies from (5.5 to 8.1) g in the present experiments, is determined with a precision of 1×10^{-4} g. The ionic liquid is kept under vacuum (approximately 10 Pa) for being degassed and dried for at least 24 h at 303 K.

The equilibrium process starts by bringing into contact the solute and the solvent by closing valve V1 and opening valve V2 or V3 (constant volume valves). The total volume of the equilibrium section was previously calibrated by gas expansions from the gas bulbs at different temperatures to appropriately take into account the thermal expansion corrections (V_{tot} = (117.10 ± 0.02) cm^3 at T = 302.39 K with a thermal expansion coefficient $\alpha = 6.51 \times 10^{-5}$). The pressure and temperature during the equilibration process are recorded in a computer until constant values are reached which means that thermodynamic equilibrium is attained.

The determination of the solubility at different temperatures is simply done by changing the liquid thermostat set points and waiting for a new thermodynamic equilibrium at a different temperature. With a single loading it is thus possible to make measurements over a large temperature range, for example, T = 298 K to T = 343 K in this study. Several runs were performed with different ionic liquid and gas fillings.

The method of data reduction was reported in previous publications.[18−20] The solubility of the gaseous solute in the ionic liquid can be expressed in mole fraction which is calculated from

$$x_2 = \frac{n_2^{liq}}{n_1^{liq} + n_2^{liq}} \quad (1)$$

where n_2^{liq} is the amount of solute dissolved in the ionic liquid and $n_1^{liq} = n_1^{tot}$ is the total amount of ionic liquid (subscript 2 stands for solute and subscript 1 for solvent).

The quantity of solute in the liquid solution is determined by the difference between two pVT measurements; first, when the gas is introduced in the equilibrium cell, and second, after thermodynamic equilibrium is reached

TABLE 1: Experimental Densities, ρ, of the Three Studied Ionic Liquids: [C₈H₄F₁₃mim][NTf₂] between 293 and 343 K up to 25 MPa; [C₈mim][NTf₂] and [C₁₀mim][NTf₂] between 293 and 343 K^a

T/K	$p/10^5Pa$	$\rho/kg\,m^{-3}$	T/K	$p/10^5Pa$	$\rho/kg\,m^{-3}$
	[C₈H₄F₁₃mim][NTf₂]			[C₈mim][NTf₂]	
293.17	1.02	1724.1(1723.3)	308.30	1.0	1314.6
293.16	2.50	1724.3	308.31	1.0	1314.8
293.17	5.03	1724.6	308.32	1.0	1314.6
293.17	10.0	1725.2	308.38	1.0	1314.9
293.17	25.0	1726.8	313.19	1.0	1309.0
293.16	50.0	1729.5	313.22	1.0	1308.9
293.15	100	1734.7	313.23	1.0	1309.1
293.14	150	1739.7	313.26	1.0	1309.1
293.13	200	1744.5	323.08	1.0	1299.9
293.11	250	1749.2	323.10	1.0	1299.8
303.17	1.03	1711.6 (1710.7)	323.10	1.0	1300.1
303.17	2.50	1711.7	323.14	1.0	1300.1
303.17	5.02	1712.0	332.87	1.0	1291.3
303.17	10.0	1712.6	332.92	1.0	1291.4
303.17	25.0	1714.3	332.93	1.0	1291.4
303.17	50.0	1717.1	333.06	1.0	1291.7
303.19	100	1722.5			
303.17	150	1727.7		[C₁₀mim][NTf₂]	
303.17	200	1732.7	308.37	1.0	1270.5
303.18	250	1737.5	308.38	1.0	1270.6
313.14	1.04	1699.1 (1698.3)	313.20	1.0	1265.1
313.14	2.55	1699.3	313.22	1.0	1264.9
313.16	5.03	1699.6	323.14	1.0	1256.3
313.18	10.0	1700.2	323.16	1.0	1256.1
313.18	25.0	1701.9	332.88	1.0	1247.6
313.18	50.0	1704.9	332.88	1.0	1247.7
313.18	100	1710.5			
313.19	150	1716.0			
313.21	200	1721.1			
313.21	250	1726.1			
323.15	1.02	1686.3 (1685.5)			
323.15	2.53	1686.5			
323.15	5.00	1686.8			
323.14	10.0	1687.5			
323.15	25.0	1689.3			
323.13	50.0	1692.5			
323.15	100	1698.3			
323.15	150	1703.9			
323.13	200	1709.4			
323.14	250	1714.5			
333.22	1.01	1673.7 (1673.0)			
333.21	2.51	1674.0			
333.19	5.02	1674.3			
333.19	10.0	1675.0			
333.19	25.0	1677.0			
333.20	50.0	1680.2			
333.20	100	1686.2			
333.19	150	1692.1			
333.19	200	1697.8			
333.21	250	1703.1			
343.18	1.00	1661.7 (1661.1)			
343.17	2.51	1662.0			
343.16	5.02	1662.3			
343.16	10.0	1663.1			
343.16	25.0	1665.1			
343.17	50.0	1668.5			
343.18	100	1674.8			
343.17	150	1681.0			
343.18	200	1686.9			
343.18	250	1692.5			

^{a} All the values are corrected for the viscosity except for [C₈H₄F₁₃mim][NTf₂] at pressures above atmospheric; the corrected values are indicated in parentheses.

$$n_2^{liq} = \frac{p_{ini}V_{GB}}{Z_2(p_{ini}, T_{ini})RT_{ini}} - \frac{p_{eq}(V_{Tot} - V_{liq})}{Z_2(p_{eq}, T_{eq})RT_{eq}} \qquad (2)$$

where V_{GB} is the volume of the bulb initially filled with the gaseous solute at temperature T_{ini}, V_{tot} is the total volume of the equilibrium cell (calibrated by gas expansions), and V_{liq} the volume occupied by the liquid solution at the equilibrium temperature T_{eq}. This volume can be measured accurately enough in the present experimental arrangement (by a gas

TABLE 2: Experimental Dynamic Viscosities, η, of [C$_8$H$_4$F$_{13}$mim][NTf$_2$], [C$_8$mim][NTf$_2$], and [C$_{10}$mim][NTf$_2$] As a Function of Temperature at Atmospheric Pressure

	η/mPa s		
T/K	[C$_8$H$_4$F$_{13}$mim][NTf$_2$]	[C$_8$mim][NTf$_2$]	[C$_{10}$mim][NTf$_2$]
293.15	1814	121.7	153.88
303.15	824.0	73.61	91.84
313.15	413.1	47.39	58.49
323.15	223.4	32.67	39.41
333.15	137.7	23.38	27.78
343.15	86.93	17.36	20.28
353.15	56.23	13.35	15.50
363.15	39.89	10.41	11.99

expansion followed by a *pVT* measurement after equilibrium) but in the present case it was obtained by considering the density of the solution as equal to that of the pure solvent. p_{ini} is the initial pressure of gaseous solute present in the gas bulb and p_{eq} the equilibrium pressure. Z_2 is the compression factor for the pure gas. Henry's law constants, considered in the present case as independent of pressure, can be calculated from the mole fraction solubilities given by eq 1 above as

$$K_{H} = \lim_{x_2 \to 0} \frac{f_2(p, T, x_2)}{x_2} = \frac{\phi_2(p_{eq}, T_{eq})p_{eq}}{x_2} \qquad (3)$$

where f_2 is the fugacity of the solute and ϕ_2 is its fugacity coefficient calculated in the usual way. The fugacity coefficient, which is very close to unity in the present cases, was included in the calculation of the Henry's law constants.

Molecular Simulation. Ionic liquids were represented by an all-atom force field of the OPLS-AA family, specifically parametrized for ionic liquids.[21,22] This model contains all the parameters required to simulate the ions C$_n$mim$^+$, NTf$_2^-$, and was recently extended[23] to functionalized ionic liquids, including the necessary parameters, such as partial atomic charges and torsion energy profiles, necessary to simulate ionic liquids containing fluorinated alkyl side chains.

The ionic liquids [C$_8$mim][NTf$_2$] and [C$_8$F$_{13}$H$_4$mim][NTf$_2$] were simulated in periodic cubic boxes containing 250 ion pairs, using the molecular dynamics method implemented in the DLPOLY package.[24] Electrostatic forces were calculated using the Ewald summation method. Starting from low-density random configurations, the systems were allowed to equilibrate at 373 K for 500 ps at constant NpT, with a time step of 2 fs. Once the equilibrium density attained, simulations runs of 500 ps were performed from which 2500 configurations were stored. Additionally, simulation boxes containing 246 ion pairs and 8 CO$_2$

molecules were prepared in the same manner to calculate solute–solvent radial distribution functions between the gas and the ionic liquid. The CO$_2$ molecule was represented by the potential model of Harris and Yung.[25]

The chemical potential of CO$_2$ in the two ionic liquids was calculated in a two-step procedure. First, a reduced-size version of the CO$_2$ molecule was produced by subtracting 1 Å from the C–O bond length and also from the Lennard-Jones diameters σ_O and σ_C. The resulting molecule is small enough so that its chemical potential can be calculated using the Widom test-particle insertion method[26] with efficient statistics; here, 10^5 insertions were attempted in each of 2500 stored configurations of the pure ionic liquids. (The difficulty with the test-particle insertion method is that free volume ionic liquids is low and spontaneously present cavities capable of accommodating a full CO$_2$ molecule are very unlikely to occur; as a result, it is very difficult in practice to calculate the chemical potential of CO$_2$ by direct test-particle insertion.) Second, a stepwise finite-difference thermodynamic integration procedure[27] is followed to calculate the free-energy difference between this initial, small version of the CO$_2$ molecule and the full-size model. The free-energy calculation was performed on six intermediate steps along a linear path connecting the intermolecular parameters (bonds and diameters) of the reduced-size and of the full-size CO$_2$ molecule. This relatively modest number of intermediate steps is adequate because the starting point of the thermodynamic integration route is not too far from the final state. If we were to calculate the chemical potential of CO$_2$ by thermodynamic integration starting from the pure solvent then more intermediate steps would be required. In our finite-difference thermodynamic integration scheme, derivatives of the total energy of the system with respect to the activation parameter were evaluated by a three-point formula with increments of 2 $\times 10^{-3}$ (finite differences, in fact). The finite differences in free energy were evaluated by a free-energy perturbation formula in the NpT ensemble.

This free-energy calculation procedure has been used before for the determination of the solubility of different gases in fluorinated solvents.[28,29,7,30]

The nature of the cavities spontaneously present in both ionic liquids, [C$_8$mim][NTf$_2$] and [C$_8$F$_{13}$H$_4$mim][NTf$_2$], was studied by calculating the distribution of cavity sizes and the free energy of cavity formation from the computer simulations. We chose to calculate the free energies of cavity formation by testing the probability of inserting hard spheres using Widom's method as described in previous publications.[4,28]
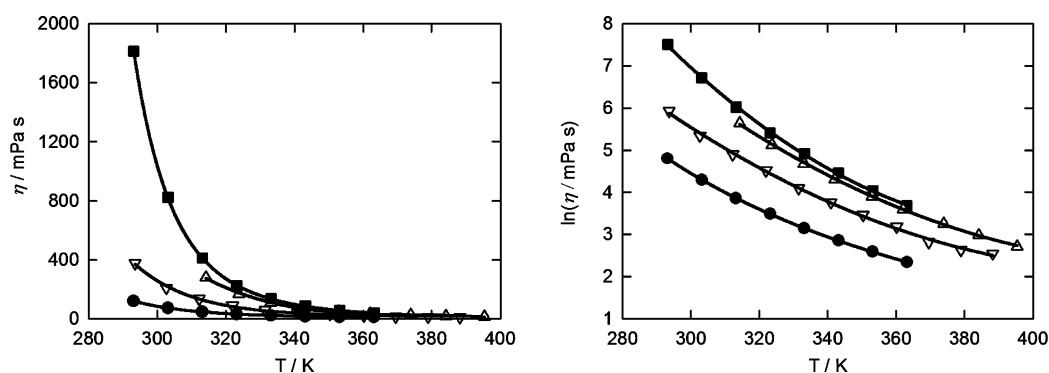
Figure 3. Experimental viscosities of several ionic liquids as a function of temperature: ■, [C$_8$H$_4$F$_{13}$mim][NTf$_2$]; △, [C$_4$mim][C$_8$SO$_4$];[47] ▽, [C$_4$mim][PF$_6$][48][2]; ●, [C$_8$mim][NTf$_2$]. The lines correspond to the fit of the data.

Fluorination and Solubility of CO$_2$ in Ionic Liquids

J. Phys. Chem. B, Vol. 114, No. 10, 2010 **3613**

Results and Discussion

The experimental values obtained for the density of [C$_8$mim][NTf$_2$] and [C$_{10}$mim][NTf$_2$] at atmospheric pressure and as a function of temperature from 283 to 333 K are reported in Table 1 together with the values for [C$_8$H$_4$F$_{13}$mim][NTf$_2$] in the same temperature range and at pressures from 0.1 to 25 MPa. The values of density at atmospheric pressure were adjusted to linear functions of temperature

$$\rho_{[C_8H_4F_{13}mim][NTf_2]}/\text{kg m}^{-3} = 2088.6 - 1246.59 \times 10^{-3}(T/K) \tag{4}$$

$$\rho_{[C_8mim][NTf_2]}/\text{kg m}^{-3} = 1602.6 - 935.66 \times 10^{-3}(T/K) \tag{5}$$

$$\rho_{[C_{10}mim][NTf_2]}/\text{kg m}^{-3} = 1554.2 - 921.68 \times 10^{-3}(T/K) \tag{6}$$

the standard deviation of the fits is always better than 0.05%. The values determined for [C$_8$mim][NTf$_2$] could be compared with those published by other authors that used vibrating tube or gravimetric density measurement techniques. Our values are on average 0.15% lower than those of Kato and Gmehling,[31] present a small systematic deviation with temperature from those of Jacquemin et al.[32] (to an average absolute deviation of 0.16% correspond values 0.3% lower than those reported here at the lower temperatures and 0.05% higher at 323 K) and are systematically higher than those of Tokuda et al.[35] (0.18% deviation on average for the temperatures studied). The density of [C$_8$H$_4$F$_{13}$mim][NTf$_2$] could be compared with that measured by other research groups using picnometric methods. The low precision reported values[33,34] are 3% higher than those found in the present work.

The dynamic viscosity was measured for the ionic liquids, previously dried, and are listed in Table 2 as a function of temperature from 293 to 363 K. The Vogel−Fulcher−Tamman (VFT) equation was used to correlate the experimental viscosities as a function of temperature of [C$_8$H$_4$F$_{13}$mim][NTf$_2$], [C$_8$mim][NTf$_2$], and [C$_{10}$mim][NTf$_2$] with a standard deviation of 0.7, 0.2, and 0.2%, respectively

$$\eta_{[C_8H_4F_{13}mim][NTf_2]}/\text{mPa s} = (2.05 \times 10^{-3}) \times (T/K)^{1/2} \exp\left[\frac{1337}{(T/K) - 170}\right] \tag{7}$$

$$\eta_{[C_8mim][NTf_2]}/\text{mPa s} = (4.03 \times 10^{-3}) \times (T/K)^{1/2} \exp\left[\frac{1005}{(T/K) - 159}\right] \tag{8}$$

$$\eta_{[C_{10}mim][NTf_2]}/\text{mPa s} = (3.43 \times 10^{-3}) \times (T/K)^{1/2} \exp\left[\frac{1080}{(T/K) - 156}\right] \tag{9}$$

In the temperature range studied, the relatively high viscosity of [C$_8$H$_4$F$_{13}$mim][NTf$_2$] decreases drastically when the temperature increases, approaching the values of the ionic liquid [C$_8$mim][NTf$_2$], which are in good agreement with literature data.[35] Effectively, at 293.15 K the viscosity of the cation−fluorinated

TABLE 3: Experimental Values of Carbon Dioxide Solubility in [C$_8$mim][NTf$_2$], in [C$_{10}$mim][NTf$_2$], and in [C$_8$H$_4$F$_{13}$mim][NTf$_2$] Expressed Both As Henry's Law Constant, K_H, and As Mole Fraction, x_2, Corrected for a Partial Pressure of Solute of 0.1 MPa^a

T/K	p/10^2 Pa	K_H/10^5 Pa	x_2/10^{-2}	dev/%
		[C$_8$mim][NTf$_2$]		
298.04	664.30	30.1	3.30	+ 1.4
298.04	664.58	30.8	3.24	− 0.7
298.04	642.60	30.6	3.25	− 0.1
303.03	681.61	33.2	3.00	+ 0.0
303.03	657.73	33.3	2.99	− 0.3
303.05	680.07	33.4	2.98	− 0.5
313.02	712.76	38.7	2.58	+ 0.9
313.02	687.18	39.1	2.54	− 0.4
313.06	710.53	39.2	2.54	− 0.5
323.00	743.71	45.0	2.21	+ 0.8
323.01	739.98	45.6	2.18	− 0.4
323.01	715.75	45.5	2.19	− 0.2
333.01	743.68	52.5	1.90	+ 0.0
333.01	769.03	52.8	1.89	− 0.5
333.02	773.96	52.1	1.91	+ 0.8
342.99	803.59	59.9	1.66	+ 0.6
343.00	797.62	60.8	1.64	− 0.9
343.01	771.16	60.2	1.66	+ 0.1
		[C$_{10}$mim][NTf$_2$]		
303.34	638.05	30.7	3.24	+ 0.0
303.40	624.51	30.8	3.23	− 0.1
313.15	665.72	36.3	2.74	+ 0.2
313.20	651.53	36.5	2.73	− 0.1
323.10	692.98	42.6	2.34	+ 0.2
323.11	677.88	42.8	2.33	− 0.1
333.09	703.88	49.9	2.00	− 0.5
333.10	719.48	49.5	2.01	+ 0.3
343.13	729.19	57.5	1.73	− 0.4
343.13	745.36	56.8	1.75	+ 0.7
343.14	729.12	57.4	1.74	− 0.2
		[C$_8$H$_4$F$_{13}$mim][NTf$_2$]		
298.04	690.43	25.3	3.93	+ 1.2
298.03	672.44	25.8	3.86	− 0.6
298.03	649.40	25.8	3.86	− 0.5
303.03	707.64	27.6	3.61	+ 1.3
303.04	688.93	28.1	3.54	− 0.6
303.02	665.18	28.1	3.54	− 0.5
303.02	686.45	28.1	3.55	− 0.4
313.02	741.38	32.6	3.06	+ 0.9
313.08	720.73	33.1	3.01	− 0.4
313.11	695.84	32.9	3.03	+ 0.1
323.02	773.94	38.0	2.62	+ 0.5
323.06	751.57	38.5	2.59	− 0.7
323.10	725.50	38.3	2.60	+ 0.0
323.05	434.62	38.4	2.59	− 0.4
333.02	804.92	43.6	2.29	+ 0.9
333.06	781.43	44.3	2.25	− 0.8
333.06	754.15	44.0	2.27	+ 0.0
343.02	835.29	49.5	2.01	+ 1.1
343.06	810.63	50.6	1.97	− 1.0
343.06	782.27	50.1	1.99	+ 0.0

^{a} p is the experimental equilibrium pressure and the percent deviation is relative to the correlations of the data reported in Table 4.

ionic liquid, is 14.8 times the viscosity of the nonfluorinated ionic liquid, decreasing to 3.8 times at 363.15 K. In Figure 3 are compared the values for the viscosity of several ionic liquids and it can be easily observed that, although [C$_8$H$_4$F$_{13}$mim][NTf$_2$] presents a relatively high viscosity, it is similar to that of ionic liquids with different anions like, for example, the [C$_4$mim][C$_8$H$_{17}$SO$_4$].[14]

TABLE 4: Parameters of Equation 10 Used to Smooth the Experimental Results on K_H from Table 3 along with the Standard Deviation of the Fit, s
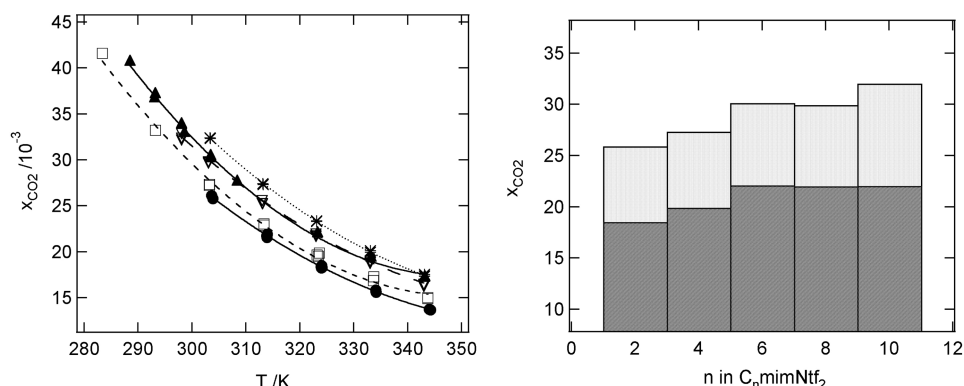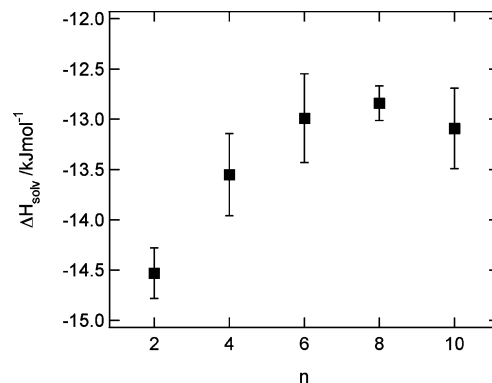
ionic liquid	A_0	A_1	A_2	s
[C$_8$mim][NTf$_2$]	+9.49	-2.117×10^3	$+9.126 \times 10^4$	0.7
[C$_{10}$mim][NTf$_2$]	+8.47	-1.422×10^3	-3.301×10^4	0.4
[C$_8$H$_4$F$_{13}$mim][NTf$_2$]	+7.32	-8.624×10^2	-1.048×10^5	0.6

For each of the ionic liquids studied, [C$_8$H$_4$F$_{13}$mim][NTf$_2$], [C$_8$mim][NTf$_2$] and [C$_{10}$mim][NTf$_2$], multiple experimental data points of the carbon dioxide solubility were obtained in the temperature interval between 298 and 343 K in steps of approximately 10 K. The experimental values, reported as mole fraction of the solute and as Henry's law constants, are reported in Table 3. These last values are calculated from the experimental data of K_H (at slightly different total pressures) assuming a partial pressure of the gaseous solute equal to 0.1 MPa. The relative atomic masses used are the ones recommended by IUPAC[36] and the values of the second virial coefficients for carbon dioxide, necessary for the calculation of the compressibility factor and of the fugacity coefficient of the solute, were taken from the compilation by Dymond and Smith.[37]

To obtain representative values of the solubility, the Henry's law constants calculated from the experimental data were adjusted to power series in $1/T$

$$\ln[K_H(T)/10^5 \, \text{Pa}] = \sum_{i=0}^{n} A_i (T/K)^{-i} \qquad (10)$$

The coefficients A_i as well as the standard deviations of the fits, considered as a measure of the precision of the data, are collected in Table 4. The Henry's law constants, calculated from the solubility measurements described in this work, are considered to be precise to within less than 1%. To estimate the accuracy of the carbon dioxide solubilities reported in Table 3, the values herein were confronted to those published by different research groups. For CO$_2$ in [C$_8$H$_4$F$_{13}$mim][NTf$_2$], Baltus et al.[10] have determined a Henry's law constant of 4.5 ± 1 bar at 298.15 K, a value inferior by 83% to the one of 25.8 ± 0.3 bar determined in this work. Our value agrees to within 6% with the one reported by Muldoon et al.[11] that have measured a Henry's law constant for CO$_2$ in [C$_8$H$_4$F$_{13}$mim][NTf$_2$] of 27.3 ± 0.2 bar at 298.15 K. The overestimation of the carbon dioxide solubility in the partially fluorinated imidazolium based ionic liquid published by Baltus et al. is particularly strange as the same authors publish a Henry's law constant of 30 ± 1 bar for

Figure 5. Enthalpies of solvation of carbon dioxide in 1-alkyl-3-methylimidazolium bis(trifluoromethylsulfonyl)amide as a function of the size of the alkyl-side chain in the cation: $n = 2$,[39,40] $n = 4$,[40] $n = 6$,[20] and $n = 8$, 10, this work.

CO$_2$ in [C$_8$mim][NTf$_2$],[10] a value that agrees with the present value of 30.5 ± 0.4 bar to within the mutual uncertainties. Muldoon et al.,[11] who have measured the solubility of CO$_2$ in [C$_8$H$_4$F$_{13}$mim][NTf$_2$] using different experimental techniques, attribute the discrepancy for the value reported by Baltus et al.[10] to the use of a quartz crystal microbalance, a technique that leads to an overestimation of the carbon dioxide solubility in this particular ionic liquid. After a careful analysis of the present data and in light of the comparisons made here, we consider that the present values have an accuracy better than ±5%.

It is observed that carbon dioxide solubility increases with the increase of the alkyl-side chain of the imidazolium cation. This effect has been already described in the literature[20,38,39] at least for imidazolium cations with alkyl-side chains up to 6 carbon atoms, but it is often considered as minor, compared with the change on solubility caused by modifying the anion of the ionic liquid. In Figure 4 shows the carbon dioxide solubility in 1-alkyl-3-methylimidazolium bis(trifluoromethylsulfonyl)amide ionic liquids with alkyl chain containing 2,[39,40] 4,[39] 6,[20] 8, or 10 carbon atoms. It is observed that although the solubility increases with the number or carbon atoms in the alkyl chain, the rise is less important for longer alkyl chains, especially above eight carbon atoms. This tendency is also reported by Chen et al.[41] for the carbon dioxide solubility in imidazolium-based tetrafluoroborate ionic liquids (with alkyl side-chains of four, six, or eight carbon atoms). To try to elucidate the reasons for this behavior, we have calculated the thermodynamic properties of solvation for carbon dioxide in the ionic liquids studied. The average values calculated for the temperature range

Figure 4. Carbon dioxide solubility in 1-alkyl-3-methylimidazolium bis(trifluoromethylsulfonyl)amide ionic liquids as a function of the number of carbon atoms, n, in the alkyl-side chain. On the left: ●, [C$_2$mim][NTf$_2$]; □, [C$_4$mim][NTf$_2$]; ▲, [C$_6$mim][NTf$_2$]; ▽, [C$_8$mim][NTf$_2$]; ∗, [C$_{10}$mim][NTf$_2$]. On the right: carbon dioxide solubility at 303 K in light gray and carbon dioxide solubility at 323 K in dark gray.

TABLE 5: Thermodynamic Functions of Solvation for CO_2 in [C$_8$mim][NTf$_2$], [C$_{10}$mim][NTf$_2$], and [C$_8$H$_4$F$_{13}$mim][NTf$_2$] in the Temperature Range Studied[a]

T/K	ΔH_{solv}/kJ mol^{-1}	ΔS_{solv}/J mol^{-1} K^{-1}
	[C$_8$mim][NTf$_2$] + CO_2	
298−343	−12.8 ± 0.2	−70.9 ± 0.2
	[C$_{10}$mim][NTf$_2$]+ CO_2	
298−343	−13.2 ± 0.3	−71.7 ± 0.8
	[C$_8$H$_4$F$_{13}$mim][NTf$_2$] + CO_2	
298−343	−12.6 ± 0.2	−69.3 ± 0.4

[a] ΔH_{solv} is the enthalpy of solvation and $\Delta_{solv}S$ the entropy of solvation.

covered in this work are listed in Table 5, the enthalpies of solvation being represented in Figure 5. It is observed that the enthalpies of solvation do not vary significantly with the length of the alkyl-side chain of the cation, the increase of solubility being explained by the balance of the carbon dioxide−ionic liquid interactions (enthalpic term) and the structure of the solvent surrounding the solute (entropic term). The negative values observed for the entropy of solvation can be explained by the structuring effect caused by the specific interactions between the solute and the charged centers of the ionic liquid, as showed previously by molecular simulation.[42]

From the results obtained in this work, we can also quantify the effect of the fluorination of the cation on the carbon dioxide solubility in ionic liquids. As observed in Figure 6 (and listed in Table 5), the solubility in the partially fluorinated ionic liquid is higher than in its hydrogenated counterpart by a factor 1.19. Molecular simulation was used to explain the molecular mechanisms of solvation in this system. First, calculation of the free energy of solvation of CO_2 in both ionic liquids, [C$_8$mim][NTf$_2$] and [C$_8$ F$_{13}$H$_4$mim][NTf$_2$] at 373 K yielded values of K_H = 86.3 ± 0.7 bar and K_H = 73.8 ± 0.6 bar, respectively, for the two ionic liquids, which correspond to x_{CO2} = (1.2 ± 0.7) × 10^{-2} and x_{CO2} = (1.4 ± 0.7) × 10^{-2} at a partial pressure p_{CO2} = 1 bar. As seen in Figure 7, these calculations agree with the experimental results to within the mutual errors for both ionic liquids. This quantitative agreement is a validation of the force field models to describe CO_2−ionic liquid interactions. Other structural and energetic properties should be correct as well.

The molecular structure of the solutions was studied by calculating the site−site solute−solvent radial distribution for the carbon dioxide solutions. Some of the most significant

differences between the fluorinated and the hydrogenated ionic liquids are plotted in Figure 7. It can be observed that carbon dioxide is solvated near different sites of the ionic liquid, depending on its degree of fluorination. In that case, carbon dioxide more likely takes position near the position C$_2$ of the imidazolium ring in [C$_8$mim][NTf$_2$] than in [C$_8$H$_4$F$_{13}$mim][NTf$_2$], although near positions C$_4$ and C$_5$ carbon dioxide are more likely found in the [C$_8$H$_4$F$_{13}$mim][NTf$_2$]. As expected, carbon dioxide shows its affinity for the fluorinated alkyl chain; the gaseous solute is more likely found near the terminal carbon of the alkyl-side chain (CTF) in the case of [C$_8$H$_4$F$_{13}$mim][NTf$_2$] when compared with [C$_8$mim][NTf$_2$] (CT).

Depending on the degree of fluorination of the alkyl side chain in the imidazolium cation, the ionic liquids adopt different conformations that surely affect their behavior as solvents. The distribution of spontaneous cavity sizes and the associated free energy of cavity formation in the ionic liquids are plotted in Figure 8. It demonstrated that the population of cavities of a given size is always larger in the ionic liquid that has a partially fluorinated cation, forming a cavity in this case always requiring less work than in the cation containing an hydrogenated alkyl-side chain, as shown by the calculated free energies of cavity formation also plotted in Figure 8.

It is expected that the increase of the fluorinated chain on the imidazolium cation would have the same effect on the carbon dioxide solubility observed for hydrogenated alkyl chains. The fluorinated alkylimidazolium cations also lead to nanostructured ionic liquids[45] as proven from the analysis of the site−site intermolecular radial distribution functions of the terminal fluorinated carbon of the ionic liquid [C$_8$H$_4$F$_{13}$mim][NTf$_2$] depicted in Figure 9 together with the function for the hydrogenated cation counterpart. The increase of the length of the fluorinated chain in the imidazolium cation will then most certainly have the same effect on the carbon dioxide solubility. The nonpolar domains of the fluorinated ionic liquid will become more important with the consequent dilution of the charged domains that are determining for the solvation of carbon dioxide.[42]

Conclusions

This work shows that it is possible to significantly increase the carbon dioxide uptake by an ionic liquid through functional groups that increase its affinity toward the gas, relying on physical interactions only. To do so, we have synthesized an octylimidazolium-based ionic liquid with six fluorinated carbon atoms of the alkyl side chain in and have observed an increase
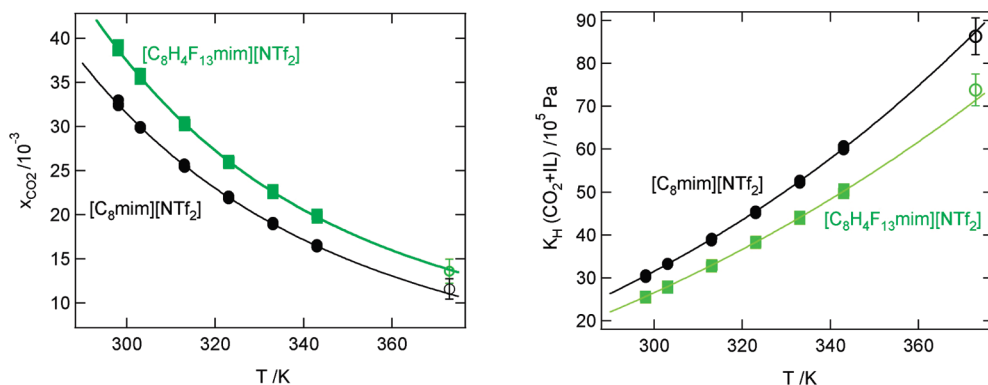

Figure 6. Effect of the partial fluorination of the cation on the carbon dioxide solubility in 1-methyl-3-octylimidazolium bis(trifluoromethylsulfonyl)amide ionic liquids as a function of temperature expressed as mole fraction of carbon dioxide at a partial pressure of 1 bar (left-hand-side plot) and as Henry's law constants (right-hand-side plot). Full symbols are experimental results and open symbols are molecular simulation calculations. ●, [C$_8$mim][NTf$_2$] and green ■, [C$_8$H$_4$F$_{13}$mim][NTf$_2$]
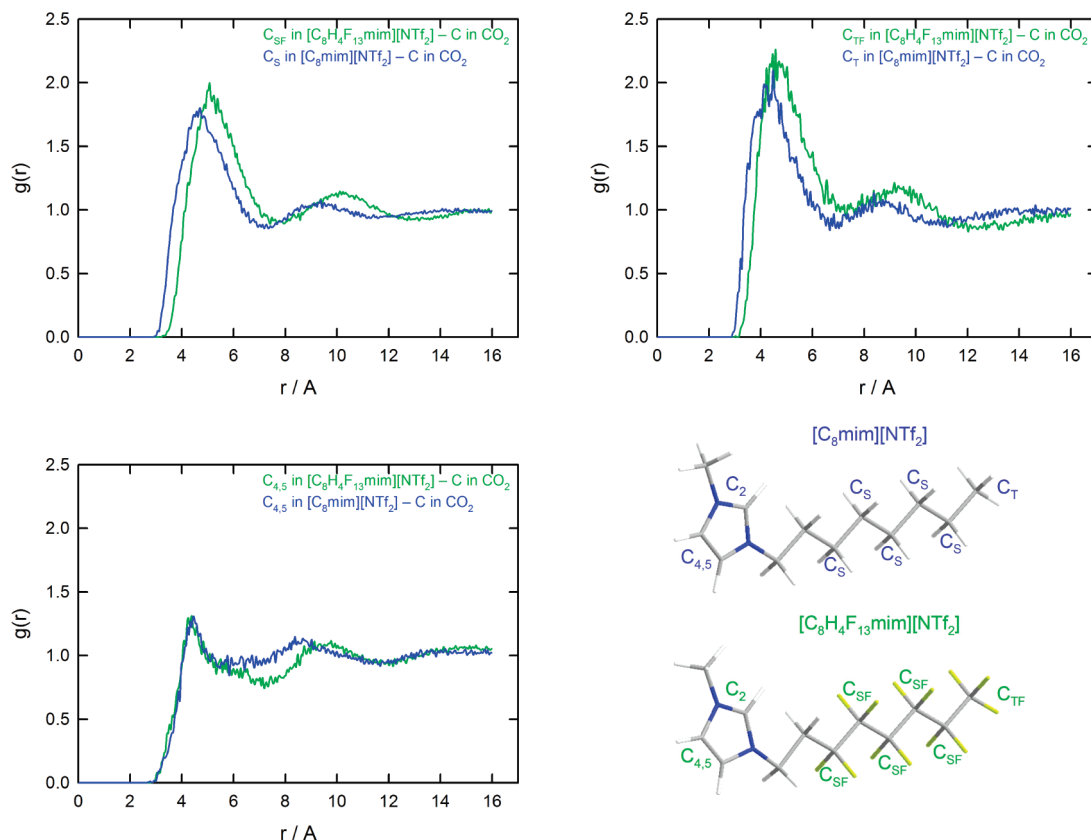
Figure 7. Solute−solvent site−site radial distribution functions of carbon dioxide in two ionic liquids. [C$_8$mim][NTf$_2$] and [C$_8$H$_4$F$_{13}$mim][NTf$_2$].
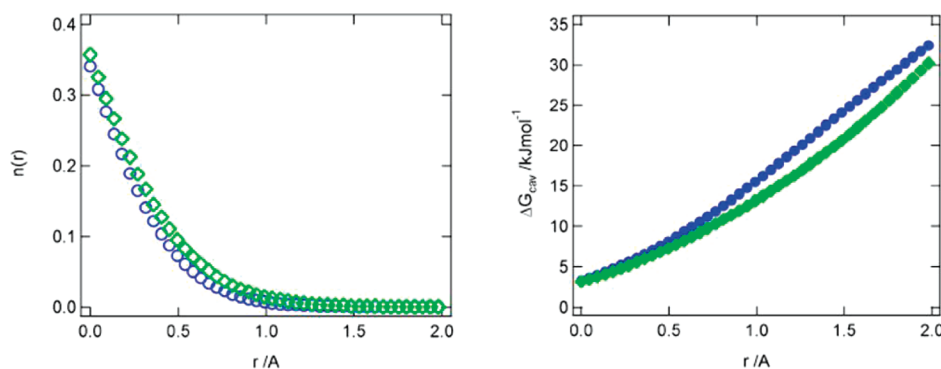

Figure 8. Distribution of the population of spontaneous cavities size (left-hand side plot) and free energy of cavity formation (right-hand side plot) in [C$_8$mim][NTf$_2$] (○,●, in blue) and in [C$_8$H$_4$F$_{13}$mim][NTf$_2$] (◇,◆, in green) at 1 bar.

of approximately 20% on the solubility of CO$_2$ at pressures close to atmospheric and at temperatures ranging from 303 to 343 K. The physical chemical properties of the ionic liquid, like the density and the viscosity, are not significantly affected by the fluorination of the alkyl-side chain of the imidazolium cation.

This increase of solubility was expected, as the affinity of carbon dioxide for fluorinated alkyl chains is known and has been explained[4] and exploited before, for example, in biomedical applications[43] or in supercritical reaction and extraction media.[44] This affinity has been attributed, on one hand, to the larger free volume in the fluorinated compounds when compared to hydrogenated counterparts and, on the other hand, to the stronger interactions of carbon dioxide with the fluorinated alkyl chains due to dispersion forces. This mechanism of solvation for carbon dioxide has been confirmed here for ionic liquids partially fluorinated in the alkyl side chain of alkylimidazolium cations and associated with bis(trifluoromethylsulfonyl)amide anions. The solubility of carbon dioxide was measured experimentally

and determined by molecular simulation in ionic liquids with fluorinated or hydrogenated alkyl-side chains and the molecular structure of the solutions was analyzed. In the case of the fluorinated ionic liquid, the gaseous solute can be solvated, not only near the charged domains,[45,46] as in the case of the 1-octyl-3-methylimidazolium based ionic liquid, but also near the fluorinated carbons of the cation.

It is tempting to think that the increase of the size of the fluorinated chain could lead to a steady augmentation of the gaseous uptake by the liquid. To clarify this point, we have studied the effect of the size of the alkyl chain in the cation on the solubility of carbon dioxide in alkylimidazolium ionic liquids. Carbon dioxide solubility increases with the increase of the number of carbon atoms of the alkyl chain in the cation, due to the increase of the van der Waals-type interactions between the gas and the liquid, the solute−solvent electrostatic interactions being approximately constant. However, the uptake of gas does not increase linearly with the length of the alkyl
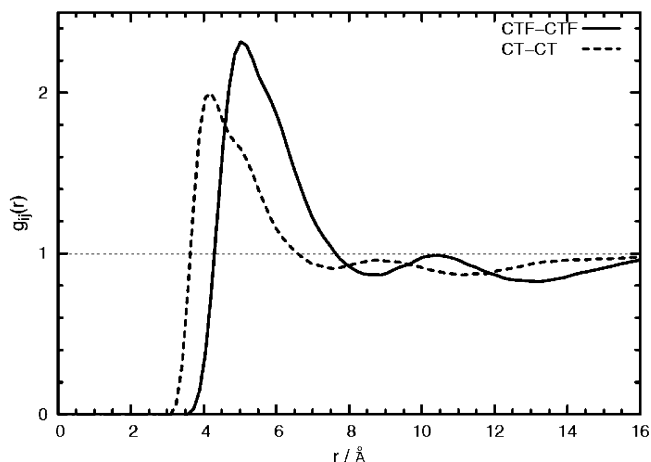
Figure 9. Site−site intermolecular radial distribution functions of the terminal carbon of the alkyl side-chain in [C$_8$mim][NTf$_2$] (dashed line) and [C$_8$H$_4$F$_{13}$mim][NTf$_2$] (solid line).

chain in the cation, its augmentation being less important for alkyl chains larger than 8 carbon atoms. Also in this case, the segregated nature of the ionic liquids, characterized by the coexistence of nonpolar domains permeated by ionic channels has to be considered to explain the solvation of the gaseous solute. For alkyl chains larger than 8 carbon atoms, the nonpolar domains probably become too large for a solute that is still preferentially solvated near the regions of the ionic liquid dominated by electrostatic interactions.

It is clear from the results presented in this work, obtained by complementing experimental data on gas solubility with molecular simulation calculations, that the intrinsic complexity of ionic liquids must always be taken into account when dealing with their ability to dissolve gases. Even if the chemical modification of the cation or the anion in the ionic liquid seem the way to go to find the most appropriate solvent for a given application, the solvation phenomena in this media needs to be interpreted in light of their complex molecular structure characterized by the coexistence of domains dominated either by electrostatic or by dispersion interactions.

Supporting Information Available: This material is available free of charge via the Internet at http://pubs.acs.org.

References and Notes

(1) Pennline, H. W.; Luebke, D. R.; Jones, K. L.; Myers, C. R.; Morsi, B. I.; Heintz, Y. J.; Ilconich, J. B. _Fluid Process. Technol._ **2008**, _89_, 897.

(2) Figueroa, J. D.; Fout, T.; Plasynski, S.; McIlvreied, H.; Srivastava, R. D. _Int. J. Greenhouse Gas Control_ **2008**, _2_, 9.

(3) Huang, J.; Ruther, T. _Aust. J. Chem._ **2009**, _62_, 298.

(4) Costa Gomes, M. F.; Pádua, A. A. H. _J. Phys. Chem B_ **2003**, _107_, 14020.

(5) Dias, A. M. A.; Bonifacio, R. P.; Marrucho, I. M.; Padua, A. A. H.; Costa Gomes, M. F. _Phys. Chem. Chem. Phys._ **2003**, _5_, 543.

(6) Costa Gomes, M. F.; Deschamps, J.; Menz, D.-H. _J. Fluorine Chemistry_ **2004**, _125_, 1325.

(7) Deschamps, J.; Costa Gomes, M. F.; Padua, A. A. H. _J. Phys. Chem B_ **2006**, _110_, 18566.

(8) Deschamps, J.; Menz, D.-H.; Padua, A. A. H.; Costa Gomes, M. F. _J. Chem. Thermodyn._ **2007**, _39_, 847.

(9) Bates, E. D.; Mayton, R. D.; Ntai, I.; Davis, J. H. J. _J. Am. Chem. Soc._ **2002**, _124_, 926.

(10) Baltus, R. E.; Culbertson, B. H.; Dai, S.; Luo, H.; DePaoli, D. W. _J. Phys. Chem. B_ **2004**, _108_, 721.

(11) Muldoon, M. J.; Aki, S. N. V. K.; Anderson, J. L.; Dixon, J. K.; Brennecke, J. F. _J.Phys. Chem. B_ **2007**, _111_, 9001.

(12) Merrigan, T. L.; Bates, E. D.; Dorman, S. C.; Davis, J. H. _Chem. Commun._ **2000**, 2051–2052.

(13) Singh, R. P.; Winter, R. W.; Gard, G. L.; Gao, Y.; Shreeve, J. M. _Inorg. Chem._ **2003**, _42_, 6142–6146.

(14) Jacquemin, J.; Husson, P.; Padua, A. A. H.; Majer, V. _Green Chem._ **2006**, _8_, 172.

(15) Jacquemin, J.; Husson, P.; Majer, V.; Cibulka, I. _J. Chem. Eng. Data_ **2007**, _52_, 2204.

(16) Schilling, G.; Kleinrahm, R.; Wagner, W. _J. Chem. Thermodyn._ **2008**, _40_, 1095–1105.

(17) Fandino, O.; Pensado, A. S.; Lugo, L.; Comunas, M. J. P.; Fernandez, J. _J. Chem. Eng. Data_ **2005**, _50_, 939–946.

(18) Jacquemin, J.; Costa Gomes, M. F.; Husson, P.; Majer, V. _J. Chem. Thermodyn._ **2006**, _38_, 490.

(19) Jacquemin, J.; Husson, P.; Majer, V.; Costa Gomes, M. F. _Fluid Phase Equilib._ **2006**, _240_, 87.

(20) Costa Gomes, M. F. _J. Chem. Eng. Data_ **2007**, _52_, 472.

(21) Canongia Lopes, J. N.; Deschamps, J.; Padua, A. A. H. _J. Phys. Chem. B_ **2004**, _108_, 2038.

(22) Canongia Lopes, J. N.; Padua, A. A. H. _J. Phys. Chem. B_ **2004**, _108_, 16893.

(23) Shimizu, K.; Almantariotis, D.; Costa Gomes, M. F.; Pádua, A. A. H.; Canongia Lopes, J. N. _J. Phys. Chem. B_, submitted for publication, **2010**.

(24) Smith, W. F., T. R., _The DL_POLY package of molecular simulation routines, Version 2.12_, Daresbury Laboratory, Warrington, U.K., 2009.

(25) Harris, J. G.; Yung, K. H. _J. Phys. Chem._ **1995**, _99_, 12021.

(26) Widom, B. J. _J. Chem. Phys._ **1963**, _39_, 2908.

(27) Mezei, M. _J. Chem. Phys._ **1987**, _86_, 7084–7088.

(28) Costa Gomes, M. F.; Pádua, A. A. H. _Pure Appl. Chem._ **2005**, _77_, 653.

(29) Deschamps, J.; Costa Gomes, M. F.; Pádua, A. A. H. _J. Fluorine Chemistry_ **2004**, _125_, 409.

(30) Podgorsek, A.; Stavber, S.; Zupan, M.; Iskra, J.; Padua, A. A. H.; Costa Gomes, M. F. _J. Phys. Chem. B_ **2008**, _112_, 6653.

(31) Kato, R.; Gmehling, J. _J. Chem. Thermodyn._ **2005**, _37_, 603.

(32) Jacquemin, J.; Ge, P.; Nancarrow, P.; Rooney, D.; Costa Gomes, M. F.; Padua, A. A. H.; Hardacre, C. _J. Chem. Eng. Data_ **2008**, _53_, 716.

(33) Singh, R. P.; Winter, R. W.; Gard, G. L.; Gao, Y.; Shreeve, J. M. _Inorg. Chem._ **2003**, _42_, 6142.

(34) Bara, J. E.; Gabriel, C. J.; Carlisle, T. K.; Camper, D.; Finotello, A.; Gin, D. L.; Noble, R. _Chem. Eng. J._ **2009**, _147_, 43.

(35) Tokuda, H.; Hayamizu, K.; Ishii, K.; Susan, M.; Watanabe, M. _J. Phys. Chem. B_ **2005**, _109_, 6103–6110.

(36) IUPAC Commission on Atomic Weights and Isotopic Abundances. _Pure Appl. Chem._ **1986**, _58_, 1677.

(37) Dymond, J. H.; Smith, E. B. _The Virial Coefficients of Pure Gases and Mixtures_; Clarendon Press: Oxford, 1980.

(38) Blanchard, L. A.; Gu, Z.; Brennecke, J. F. _J. Phys. Chem. B_ **2001**, _105_, 2437.

(39) Jacquemin, J.; Husson, P.; Majer, V.; Costa Gomes, M. F. _J. Solution Chem._ **2007**, _36_, 967.

(40) Hong, G.; Jacquemin, J.; Husson, P.; Costa Gomes, M. F.; Deetlefs, M.; Nieuwenhuyzen, M.; Sheppard, O.; Hardacre, C. _Ind. Eng. Chem. Res._ **2006**, _45_, 8180.

(41) Chen, Y.; Zhang, S.; Yuan, X.; Zhang, Y. M.; Zhang, X.; Dai, W.; Mori, R. _Thermochim. Acta_ **2006**, _441_, 42.

(42) Deschamps, J.; Costa Gomes, M. F.; Pádua, A. A. H. _Chem. Phys. Chem._ **2004**, _5_, 1049.

(43) Riess, J. G. _Chem. Rev._ **2001**, _101_, 2797.

(44) Johnston, K. P.; Harrison, K. L.; Clarke, M. J.; Howdle, S. M.; Heitz, M. P.; Bright, F. V.; Carlier, C.; Randolph, T. W. _Science_ **1996**, _271_, 624.

(45) Canongia Lopes, J. N.; Padua, A. A. H. _J. Phys. Chem. B_ **2006**, _110_, 3330.

(46) Canongia Lopes, J. N.; Costa Gomes, M. F.; Padua, A. A. H. _J. Phys. Chem. B_ **2006**, _110_, 16816.

(47) Jacquemin, J.; Husson, P.; Majer, V.; Padua, A. A. H.; Gomes, M. F. C. _Green Chem._ **2008**, _10_, 944.